

FACTOR ANALYSIS FOR FORCED AND MIXED CONVECTION LAMINAR HEAT TRANSFER IN A HORIZONTAL TUBE USING ARTIFICIAL NEURAL NETWORK

L. M. Tam

(1) Department of Electromechanical Engineering,
Faculty of Science and Technology, University of
Macau, Av. Padre Tomás Pereira, Taipa, Macau, China.
(2) Institute for the Development and Quality, Macau,
University of Macau, Av. Padre Tomás Pereira, Taipa,
Macau, China.

fstlmt@umac.mo

**H. K. Tam, Department of Electromechanical
Engineering, Faculty of Science and Technology,
University of Macau, Av. Padre Tomás Pereira, Taipa,
Macau, China.**
hktam@umac.mo

ABSTRACT

Artificial neural network (ANN) has shown its superior predictive power compared to the conventional approaches in many studies. However, it has always been treated as a "black box" because it provides little explanation on the relative influence of the independent variables in the prediction process. In our previous work (Tam et al., 2006), an index of contribution extracted from the ANN correlation was primarily introduced to analyze the relative importance of the associated independent variables on our forced convective turbulent heat transfer data in a horizontal tube (Ghajar and Tam, 1994). The most and the least important variables were determined quantitatively and found to be thoroughly conforming to the empirical correlation and physical phenomena. In this study, we have extended the method to a more complicated data set, forced and mixed convection developing laminar flow in a horizontal tube with uniform wall heat flux. The parameters influencing the Nusselt number for this data set were Reynolds number, Grashof number, Prandtl number, the length-to-diameter ratio, and the bulk-to-wall viscosity ratio. Due to the complexity of the problem it is difficult to determine the influence of the individual independent variables. According to literature, for laminar heat transfer involving entrance and mixed convection effects, Rayleigh number and Graetz number are both important. Through the re-arrangement of those

**A. J. Ghajar, School of Mechanical and Aerospace
Engineering, Oklahoma State University, Stillwater,
Oklahoma, 74048, USA.**
ghajar@ceat.okstate.edu

**S. C. Tam, Department of Mathematics, Faculty of
Science and Technology, University of Macau, Av.
Padre Tomás Pereira, Taipa, Macau, China.**
fstsct@umac.mo

variables, the factor analysis clearly showed that the Rayleigh number has a significant influence on the mixed convection heat transfer data and the forced convection heat transfer data is more influenced by the Graetz number. The results clearly indicate that the factor analysis method can be used to provide an insight into the influence of different variables or a combination of them on complicated heat transfer problems.

INTRODUCTION

Heat transfer inside horizontal tubes in the laminar, transitional and turbulent flow regimes have been studied experimentally by various researchers in the past. Usually, the experimental results are presented in the form of heat transfer correlations. The form of the correlations is based either on different theoretical models or they are completely empirical based. The coefficients of the correlations are usually determined by the conventional least squares method. Recently Tam and Ghajar (2006) documented some of the most well accepted correlations in the above-mentioned flow regimes. A new correlation in the transition region based on the method of artificial neural network (ANN) with excellent accuracy was proposed by Ghajar et al. (2002). In their paper, it was mentioned that ANN can also be used in the determination of the most and the least important variables using the coefficient matrices obtained from the weight and bias matrices of the

ANN correlation. However, there are some unanswered questions regarding this technique, such as (1) applicability of this technique to other data sets and (2) besides the most important variables, i.e., the normalized Reynolds and Grashof numbers, and the least important variables, i.e., the normalized Sieder and Tate factor (μ_b/μ_w)^{0.14}, the importance of the normalized Prandtl number can not be seen. Recently, Tam et al. (2006) modified the method and defined an index of contribution to examine a set of experimental data in the turbulent flow region (Ghajar and Tam, 1994). It was found that the Reynolds (Re) and the Prandtl (Pr) numbers are observed as the most important parameters. The length-to-diameter ratio (x/D) and the viscosity ratio (μ_b/μ_w)^{0.14} are found to be the least important parameters. The findings are consistent with the physical meanings of the turbulent heat transfer pipe flow problems. In general, the contributions from different parameters are relatively easy to observe in the turbulent region because the turbulent motion effects are strong but the effects of entrance, buoyancy, and variation of properties are usually less significant. On the contrary, the entrance effect, the buoyancy, and the variation of physical properties in the laminar flow region are extremely important. Therefore, in this study, we will further investigate the modified method by applying it to the forced and mixed convection developing laminar flow in a horizontal tube with uniform wall heat flux in order to verify its applicability.

NOMENCLATURE

a = output vector
b = bias matrix
c_p = specific heat at constant pressure, kJ/(kg-K)
D = inside diameter of the tube, m
f = activation (or transfer) function
g = acceleration of gravity, m/s²
Gr = local bulk Grashof number (= $g\beta\rho^2D^3(T_w-T_b)/\mu^2$)
Gz = local Graetz number (= RePrD/x)
h_t = local peripheral heat transfer coefficient at the top of tube, W/(m²-K)
h_b = local peripheral heat transfer coefficient at the bottom of tube, W/(m²-K)
k = thermal conductivity, W/(m²-K)
Nu = local average or fully developed peripheral Nusselt number (= hD/k)
Nu_l = local average or fully developed peripheral laminar Nusselt number
Nu_t = local average or fully developed peripheral turbulent Nusselt number
p = input vector
P_j = contribution of the jth independent variable, p_j
Q_k = contribution of the kth neuron output to the ANN model
Pr = local bulk Prandtl number (= c_pμ_b/k)
Ra = local bulk Rayleigh number (= GrPr)
Re = local bulk Reynolds number (= ρVD/μ)
T_b = local bulk temperature, °C
T_w = local wall temperature, °C

V = average velocity in the test section, m/s

W = weight matrix

x = local distance along the test section from the inlet, m

Greek symbols

μ_b = local bulk dynamic viscosity, Pa-s
μ_w = local wall dynamic viscosity, Pa-s
ρ = density, kg/m³

Subscripts

i = dummy parameter
j = the jth input variable
k = the kth hidden neuron
max = maximum value
min = minimum value
R = number of inputs
S = number of hidden neurons

Superscripts

1 = the hidden layer of the ANN model
2 = the output layer of the ANN model

EXPERIMENTAL DATASET

The heat transfer experimental data used in this study, along with a detailed description of the experimental apparatus and procedures used, were reported by Ghajar and Tam (1994). A schematic of the overall experimental setup used for heat transfer measurements is shown in Figure 1. In this paper, only a brief description of the experimental setup and procedures will be provided. The local forced and mixed convective measurements were made in a horizontal, electrically heated, stainless steel circular straight tube with re-entrant, square-edged, and bell-mouth inlets under a uniform wall heat flux condition. The pipe had an inside diameter of 1.58 cm and an outside diameter of 1.90 cm. The total length of the test section was 6.10 m, providing a maximum length-to-diameter ratio of 385. A uniform wall heat flux boundary condition was maintained by a dc arc welder. Thermocouples (T-type) were placed on the outer surface of the tube wall at close intervals near the entrance and at greater intervals further downstream. Twenty-six axial locations were designated, with four thermocouples placed at each location. The thermocouples were placed 90 degrees apart around the periphery. From the local peripheral wall temperature measurements at each axial location, the inside wall temperatures and the local heat transfer coefficients were calculated (Ghajar and Kim, 2006). In these calculations, the axial conduction was assumed negligible (RePr > 4,200 in all cases), but peripheral and radial conduction of heat in the tube wall were included. In addition, the bulk fluid temperature was assumed to increase linearly from the inlet to the outlet. As reported by Ghajar and Tam (1994), the uncertainty analyses of the overall experimental procedures showed that there is a maximum of 9% uncertainty for the heat transfer coefficient calculations. Moreover, the heat balance error for each experimental run indicates that in general,

the heat balance error is less than 5%. For Reynolds numbers lower than 2500 where the flow is strongly influenced by secondary flow, the heat balance error is slightly higher (5–8%) for that particular Reynolds number range. To ensure a uniform velocity distribution in the test fluid before it entered the test section, the flow passed through calming and inlet sections. The calming section had a total length of 61.6 cm and consisted of a 17.8 cm diameter acrylic cylinder with three perforated acrylic plates, followed by tightly packed soda straws sandwiched between galvanized steel mesh screens.

Before entering the inlet section, the test fluid passed through a fine mesh screen and flowed undisturbed through 23.5 cm of a 6.5 cm-diameter acrylic tube before it entered the test section. The inlet section had the versatility of being modified to incorporate a re-entrant or bell-mouth inlet (see Figure 2). The re-entrant inlet was simulated by sliding 1.93 cm of the tube entrance length into the inlet section, which was otherwise the square-edged (sudden contraction) inlet. For the bell-mouth inlet, a fiberglass nozzle with a contraction ratio of 10.7 and a total length of 23.5 cm was used in place of the inlet section. In the experiments, distilled water and mixtures of distilled water and ethylene glycol were used. They collected 1290 experimental data points, and their experiments covered a local bulk Reynolds number range of 280 to 49000, a local bulk Prandtl number range of 4 to 158, a local bulk Grashof number range of 1000 to 2.5×10^5 , and a local bulk Nusselt number range of 13 to 258. The wall heat flux for their experiments ranged from 4 to 670 kW/m².

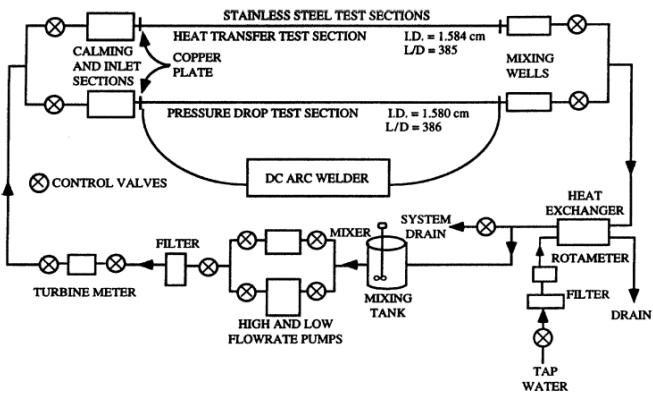


Figure 1: Schematic diagram of experimental setup.

HEAT TRANSFER CHARACTERISTICS IN THE LAMINAR AND TURBULENT REGIONS

Before analyzing the heat transfer data, it is important to review the heat transfer characteristics of the flow in the laminar and turbulent regions.

Application of heat to the tube wall produces a temperature difference in the fluid. The fluid near the tube wall has a higher temperature and lower density than the fluid close to the centerline of the tube. This temperature difference may produce a secondary flow (vortex-like flow) due to free convection. The boundary between the mixed and forced convection, according

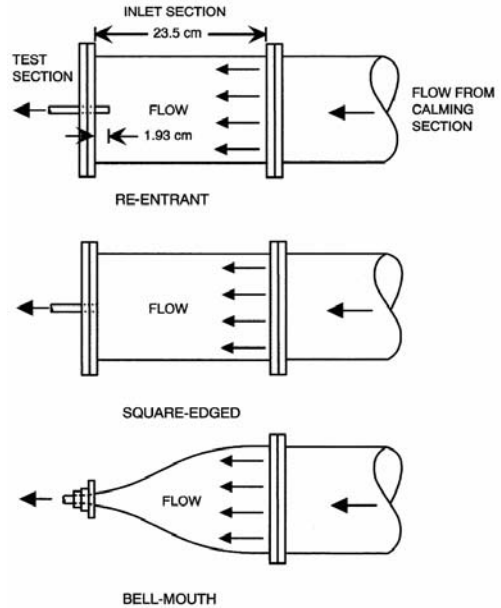


Figure 2: Schematic of the three different inlet configurations.

to Ghajar and Tam (1995), can be determined from the local peripheral heat transfer coefficient at the top of the tube to the local peripheral heat transfer coefficient at the bottom of the tube (h_t/h_b). The ratio should be close to unity (0.8–1.0) for forced convection and is much less than unity (< 0.8) for a case in which mixed convection exists. To illustrate the different heat transfer modes (mixed and forced convection) encountered for the three inlets during the experiments, Figure 3 is presented. This figure shows the effect of secondary flow on heat transfer coefficient ratio, h_t/h_b for different inlets, flow regimes, and the length-to-diameter ratio (distance from the inlet). It includes representative Reynolds number ranges from laminar to fully turbulent flow ($Re = 280\text{--}49,000$) for the three inlets. As shown in the figure, the boundary between the forced and mixed convection heat transfer is inlet-dependent. For the re-entrant, square-edged, and bell-mouth inlets when the Reynolds numbers were greater than 2500, 3000, and 8000, respectively, the flows were dominated by forced convection heat transfer and the heat transfer coefficient ratios (h_t/h_b) did not fall below 0.8–0.9 and at times exceeded unity due to the roundoff errors in the property evaluation subroutine of their data reduction program (Ghajar and Kim, 2006). However, the free convection effect was observed more significant for the low Reynolds number flows than for those in high Reynolds number. For the low Reynolds number flows dominated by mixed convection heat transfer, the h_t/h_b ratio began near 1 at the tube entrance, indicating that the flow was initially dominated by the forced convection, but dropped off rapidly as the length-to-diameter ratio (x/D) increased. Beyond about 125 diameters from the entrance, the ratio was almost invariant with x/D , indicating a much less dominant role for forced convection heat transfer and an increased free convection activity.

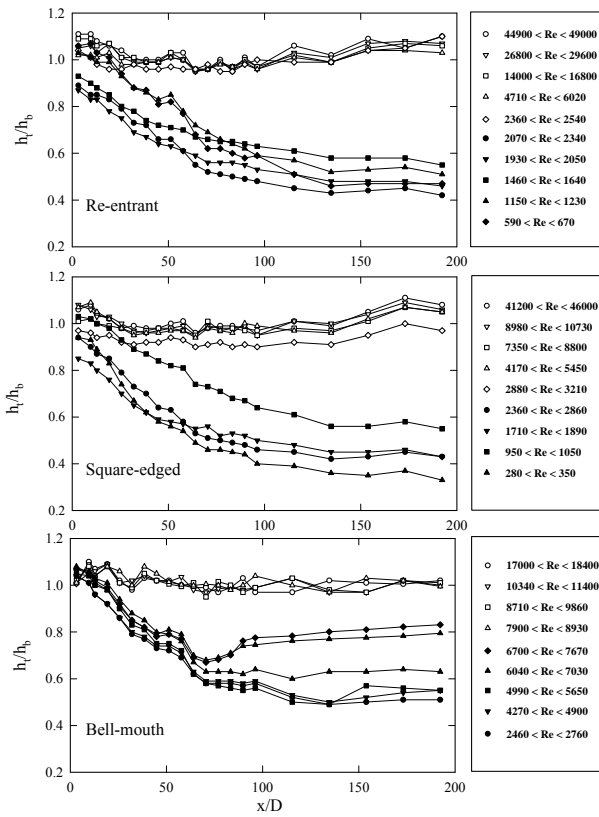


Figure 3: Effect of secondary flow on heat transfer coefficient for different inlets and flow regimes.

Based on the above observations, mixed convection only appeared in the laminar heat transfer data. Therefore, it can be concluded that the laminar Nusselt number is a function of five dimensionless variables, which are Re , Pr , Gr , x/D , and μ_b/μ_w . The ranges of these variables considered in this study for laminar flow are:

$$\begin{aligned} 13 \leq Nu &\leq 65 & ; & 280 \leq Re \leq 3800 \\ 40 \leq Pr &\leq 160 & ; & 1000 \leq Gr \leq 2.8 \times 10^4 \\ 3 \leq x/D &\leq 192 & ; & 1.2 \leq \mu_b/\mu_w \leq 3.8 \end{aligned}$$

A total of 546 experimental data points is used. Out of them, 168 data points are for the re-entrant inlet, 294 data points are for the square-edged inlet, and 84 data points are for the bell-mouth inlet. Ghajar and Tam (1994) correlated their experimental data for the laminar forced and mixed convection in the entrance and fully developed flow regions for all three inlets in the following form:

$$Nu_1 = 1.24 \left[(RePrD/x) + 0.025(GrPr)^{0.75} \right]^{1/3} (\mu_b/\mu_w)^{0.14} \quad (1)$$

The form of the above correlation is similar to the one proposed by Martinelli and Boelter (1942). The accuracy of the

correlation is described in Table 1. The majority (86%) of the laminar data were predicted by this correlation within $\pm 10\%$ deviation.

Regarding the turbulent region, the turbulent Nusselt number is a function of the dimensionless variables, Re , Pr , x/D , and μ_b/μ_w . Unlike the laminar region, Gr is not considered here since the buoyancy effect is not important in the turbulent region. The ranges of the dimensionless variables considered in this study for turbulent flow are summarized as follows:

$$\begin{aligned} 52.3 \leq Nu &\leq 242.4 & ; & 7,000 \leq Re \leq 49,000 \\ 4.0 \leq Pr &\leq 34.0 & ; & 3.21 \leq x/D \leq 173.08 \\ 1.1 \leq \mu_b/\mu_w &\leq 1.7 & & \end{aligned}$$

Ghajar and Tam (1994) developed the following correlation for their turbulent forced convection data in the entrance and fully developed regions for all three inlets:

$$Nu_t = 0.023Re^{0.8}Pr^{0.385}(x/D)^{-0.0054}(\mu_b/\mu_w)^{0.14} \quad (2)$$

A total of 604 data points were used to develop the above correlation, correlating 100% of experimental data with less than $\pm 11\%$ deviation and 73% of measured data with less than $\pm 5\%$ deviation. The details are also shown in the Table 1.

Table 1: Prediction Results for Correlations (1) & (2)

Laminar Flow Data Prediction				
Inlet Configuration	No. of Data within $\pm 10\%$	No. of Data within $\pm 5\%$	Abs. Mean Dev. (%)	Range of Dev. Abs. (%)
Total data points All three inlets (546 pts.)	466	261	5.81	-16.8% to +15.4%
Re-entrant (168 pts.)	155	94	5.01	-16.8% to +9.6%
Square-edged (294 pts.)	243	140	5.90	-16.5% to +15.4%
Bell-mouth (84 pts.)	68	27	7.08	-15.0% to +2.0%
Turbulent Flow Data Prediction				
Inlet Configuration	No. of Data within $\pm 10\%$	No. of Data within $\pm 5\%$	Abs. Mean Dev. (%)	Range of Dev. Abs. (%)
Total data points All three inlets (604 pts.)	600	439	4.42	-10.28% to 10.6%
Re-entrant (271 pts.)	269	192	3.89	-9.17% to 10.6%
Square-edged (207 pts.)	206	153	3.56	-8.74% to 10.1%
Bell-mouth (126 pts.)	125	94	3.48	-10.28% to 4.08%

FACTOR ANALYSIS METHOD

In a previous study, Tam et al. (2006) developed a factor analysis by extracting the knowledge from the “matrices weights” of the ANN correlation. The index of contribution was defined to quantify the contribution of each input variable

to the ANN. Before applying the method to the laminar dataset, the turbulent data will be examined as an illustrative example.

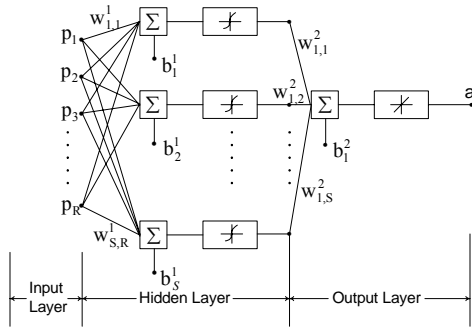


Figure 4: The three-layer ANN with S neurons in its hidden layer.

The three-layer feed-forward neural network was employed as the architecture. The schematic diagram of the network is represented in Figure 4. It has been shown that any continuous function can be modeled by the network (Hornik, 1991). The weight and the bias of the optimal ANN model are usually determined by the back propagation algorithms (Rumelhart et al., 1986). In order to determine the contribution of each independent variable to the correlation, the matrix form of the optimal ANN model has to be examined as follows:

$$N(p_1, \dots, p_R) = [w^2_1, \dots, w^2_S] \begin{bmatrix} f(\sum_{j=1}^R w^1_{1j} p_j + b^1_1) \\ f(\sum_{j=1}^R w^1_{2j} p_j + b^1_2) \\ \vdots \\ f(\sum_{j=1}^R w^1_{sj} p_j + b^1_s) \end{bmatrix} + b^2 \quad (3)$$

where (p_1, \dots, p_R) are the R inputs, S is the number of hidden neurons, $f(t) = \frac{1}{1+e^{-t}}$ is the transfer function and w 's and b 's are the weights and biases of the ANN, respectively. The contribution of the independent variables p_j to the output of the k^{th} neuron in the hidden layer $f(\sum_{j=1}^R w^1_{kj} p_j + b^1_k)$ is simply $|w^1_{kj}|$ and the relative contribution of the k^{th} neuron output to the ANN model is:

$$Q_k = \frac{|w^2_k|}{\sum_{i=1}^S |w^2_i|} \quad (4)$$

Therefore, the contribution of the independent variables p_j to the ANN model is:

$$P_j = \sum_{k=1}^S Q_k * |w^1_{kj}| \quad (5)$$

Finally, in order to compare with the other independent variables, the index of contribution of p_j is defined to be

$$\text{index}(p_j) = \frac{P_j}{\sum_{i=1}^R P_i} \times 100\% \quad (6)$$

Hence, the most significant independent variable would have the largest index of contribution. On the other hand, the variable with small index appears to be less important.

Using the supervised three-layer feed-forward neural network with fully weighted connection and the algorithm described above to determine the index of contribution for each independent variable, the stable steepest descent algorithm was selected as the best gradient method (see Tam et al., 2006). Regarding to the number of hidden neurons and training iterations employed, it was determined by the observations of the computation based on their different combinations. According to the Equation (2), the Re, Pr, x/D , and μ_b/μ_w were treated as the input variables and the Nu was used as the output variable for the training of ANN. As depicted in Figure 5, it is apparent that the index of contribution is consistent at the beginning of the 10,000 iterations regardless of the number of neurons. The index of Re and Pr numbers were close to 40% but the both ratios contributed less than 20%.

Observations can also be made using Equation (2). From Equation (2) and the range of variables mentioned in the previous section, it is obvious that Reynolds and Prandtl numbers are both important. However, it is not possible to tell which one is more important than the other by simply judging the exponents of them. It is also obvious that x/D , and μ_b/μ_w are the least important variables. According to the range of the data, the value of the terms $(x/D)^{-0.0054}$ and $(\mu_b/\mu_w)^{0.14}$ in Equation (2) are forced to a value very close to one; hence they made less contribution to the Nusselt number. Theoretically, for turbulent flow, the thermal entry length is usually very short and the entrance effect is insignificant. Moreover, from Sieder and Tate (1936), the data in the turbulent region show little variation between μ_b and μ_w , firstly, because fluids which give turbulent flow seldom have a large temperature coefficient of viscosity and secondly, because the heat transfer rates are high, preventing large temperature differences. Therefore, both the terms $(x/D)^{-0.0054}$ and $(\mu_b/\mu_w)^{0.14}$ act as correction factors to make the correlation more accurate. In consequence, the results are absolutely identical to the physical phenomena and the observations from Equation (2).

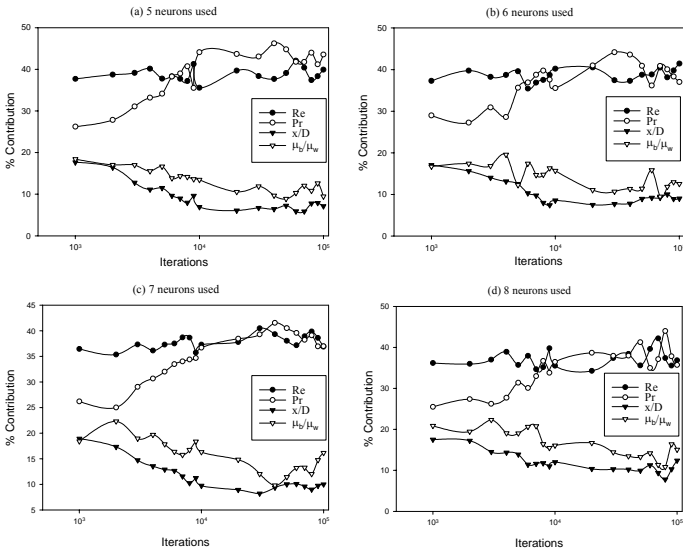


Figure 5: The percent contribution from ANN training for different dimensionless numbers to Nusselt number by adjusting the iterations and the number of neurons; (a) 5 neurons, (b) 6 neurons, (c) 7 neurons, (d) 8 neurons. Each data point is the average value from 10 trainings.

EXTENDED ANALYSIS IN LAMINAR FLOW REGION

The data in the laminar region is more complicated since the entrance effect, buoyancy and variation of properties are all important. Based on Figure 3, it is obvious that, regardless of which inlet configuration used, secondary flow requires a certain length to develop. Therefore, we can classify that the developing flow near the entrance is dominated by forced convection. When the flow is further down stream, mixed convection is the dominant mode of convection. Because of that, it would be reasonable for us to consider the first dimensionless number group, $RePrD/x$, in Equation (1) as the Graetz number to take care of the forced convection heat transfer in the thermally developing region. The second dimensionless group, $GrPr$, in Equation (1) by definition is the Rayleigh number, Ra , which is a dimensionless number considering the effect of free convection. Careful observation of Equation (1) reveals that the formation of the equation is in fact the superposition of a forced and a free convective heat transfer correlation. For the last dimensionless group, the viscosity ratio term is for the correction of the variation of physical properties due to heating. Since the wall-to-bulk temperature difference is much higher in the laminar region, this term is also important. Therefore, Equation (1) becomes:

$$Nu_1 = 1.24 \left[(Gz) + 0.025(Ra)^{0.75} \right]^{1/3} (\mu_b/\mu_w)^{0.14} \quad (7)$$

The advantages of the above arrangement are (1) the physical meanings of the dimensionless parameters are more clear and (2) the factor analysis procedures can be simplified because of the number of dimensionless variables to be

considered reduces from 5 to 3. Therefore, our factor analysis regarding the contributions from different dimensionless numbers in convective heat transfer is based on Gz , Ra and μ_b/μ_w . As shown in Figure 3, at small length-to-diameter ratios (near the tube entrance), the free convection is still not established and the flow is dominated by the forced convection based on the heat transfer coefficient ratios ($h_t/h_b > 0.8$). Therefore, the Ra number is relatively not important for the heat transfer in that region. However, as the length-to-diameter ratio is increased (20-70 diameters passed the tube entrance depending on the inlet configuration), the heat transfer mode is dominated by mixed convection and Ra number becomes an important parameter.

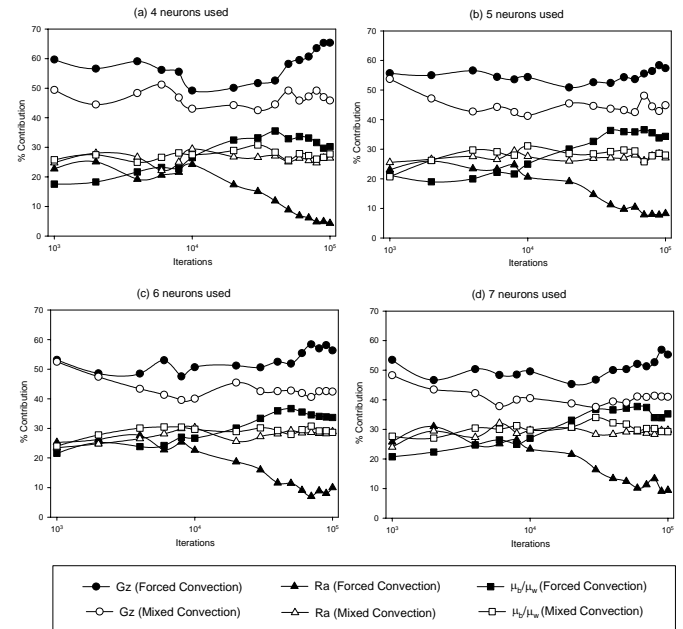


Figure 6: The percent contribution from ANN training for different dimensionless numbers to Nusselt number by adjusting the iterations and the number of neurons for forced and mixed convection; (a) 4 neurons, (b) 5 neurons, (c) 6 neurons, (d) 7 neurons. Each data point is the average value from 10 trainings.

For the analysis of the laminar flow data, a total of 546 data points from three different inlet configurations are divided into two sets, namely forced convection data with $h_t/h_b > 0.8$ and mixed convection data with $h_t/h_b < 0.8$. Out of the 546 data points, 212 data points are for the forced convection and the remaining data points are for the mixed convection. In the ANN training, the gradient method, number of hidden neurons employed, and the number of iterations used are necessary to be determined. In accordance with the analysis for the turbulent data, the steepest descent gradient algorithm gives consistent results so it was also used for the laminar data. For determination of the number of iterations and hidden neurons, the data sets were trained with 4 to 7 neurons. The number of

iterations for each training ranged from 1,000 to 100,000 times. The increment of iterations is set as 2,000 when the number of iterations is from 1,000 to 10,000. The increment of the iterations is set as 10,000 when the number of iterations is from 10,000 to 100,000. As shown in Figure 6, the trend of the contribution of each variable is consistent regardless of how many hidden neurons are employed. After 50,000 iterations, the contribution curves of each variable are very well established.

In summary, based on the observations made above, the number of iterations used is selected as 50,000 and the number of neurons used is arbitrarily selected as 6. Moreover, the form of the ANN correlation is given by Equation (3). With the establishment of the ANN correlation, the index of contribution according to the above mentioned criteria can then be computed. For reliability purposes, ninety percent of the total data points were used for training and the remaining data is for verification. The initial value of the free parameters (weights and biases) is randomly selected within ± 1 . For satisfying the log-sigmoid transfer function, the normalized input variables; Reynolds number, Prandtl number, length-to-diameter ratio, and viscosity ratio are arranged into the input vector, \mathbf{p} :

$$\mathbf{p} = \begin{bmatrix} G_z \text{ normal} \\ Ra \text{ normal} \\ \left(\frac{\mu_b}{\mu_w}\right) \text{ normal} \end{bmatrix} = \begin{bmatrix} 2 \cdot \left[G_z - G_z_{\min} \right] / \left[G_z_{\max} - G_z_{\min} \right] - 1 \\ 2 \cdot \left[Ra - Ra_{\min} \right] / \left[Ra_{\max} - Ra_{\min} \right] - 1 \\ 2 \cdot \left[\left(\frac{\mu_b}{\mu_w} \right) - \left(\frac{\mu_b}{\mu_w} \right)_{\min} \right] / \left[\left(\frac{\mu_b}{\mu_w} \right)_{\max} - \left(\frac{\mu_b}{\mu_w} \right)_{\min} \right] - 1 \end{bmatrix}$$

In Equation (3), the dependent output is the Nusselt number for the turbulent heat transfer data. The \mathbf{w}^1 , \mathbf{w}^2 , \mathbf{b}^1 , \mathbf{b}^2 terms used in Equation (3) are constant matrices or scalars. Their numerical values are shown in the followings:

For forced convection:

$$\mathbf{w}^1 = \begin{bmatrix} -3.20 & 0.12 & 1.09 \\ 1.06 & 0.31 & 1.45 \\ 0.17 & 0.49 & 2.24 \\ -0.55 & 0.58 & 0.12 \\ -0.66 & 0.11 & -0.47 \\ 0.56 & 0.71 & -0.28 \end{bmatrix}, \quad \mathbf{w}^2 = [-3.18 \ 1.14 \ 1.37 \ -1.05 \ -0.47 \ 0.09]$$

$$\mathbf{b}^1 = \begin{bmatrix} -3.45 \\ 0.32 \\ -0.34 \\ -0.31 \\ 0.30 \\ 0.29 \end{bmatrix}, \quad \mathbf{b}^2 = 0.45$$

For mixed convection:

$$\mathbf{w}^1 = \begin{bmatrix} -3.20 & 0.12 & 1.09 \\ 1.06 & 0.31 & 1.45 \\ 0.17 & 0.49 & 2.24 \\ -0.55 & 0.58 & 0.12 \\ -0.66 & 0.11 & -0.47 \\ 0.56 & 0.71 & -0.28 \end{bmatrix}, \quad \mathbf{w}^2 = [-3.18 \ 1.14 \ 1.37 \ -1.05 \ -0.47 \ 0.09]$$

$$\mathbf{b}^1 = \begin{bmatrix} 2.30 \\ -0.73 \\ -1.02 \\ -1.20 \\ -0.36 \\ 0.04 \end{bmatrix}, \quad \mathbf{b}^2 = -0.17$$

As shown in Table 2, the total number of data points for forced convection is predicted within -12.19% to 16.96% and those for mixed convection are predicted within -11.12% to 8.51%. Over 97% of the data are predicted within $\pm 10\%$ deviation for the two convection modes. For forced convection, about 77% of all the data (164 data points) are predicted within $\pm 5\%$ deviation and the absolute mean deviation is 3.56%. For the mixed convection, about 92% of all the data (308 data points) are predicted within $\pm 5\%$ deviation and the absolute mean deviation is 2.4%. As compared to the previous laminar correlation, significant improvement is observed (see Table 1).

Table 2: Prediction Results for the Improved Correlation by Using ANN

Forced Convection				
Data Point Distribution	No. of Data within $\pm 10\%$	No. of Data within $\pm 5\%$	Abs. Mean Dev. (%)	Range of Dev. Abs. (%)
Total data points (212 pts.)	207	164	3.56	-12.19% to 16.96%
Training data points (191 pts.)	186	147	3.57	-12.19% to 16.96%
Testing data points (21 pts.)	21	16	3.63	-7.70% to 9.58%
Mixed Convection				
Data Point Distribution	No. of Data within $\pm 10\%$	No. of Data within $\pm 5\%$	Abs. Mean Dev. (%)	Range of Dev. Abs. (%)
Total data points (334 pts.)	333	308	2.40	-11.12% to 8.51%
Training data points (300 pts.)	299	279	2.40	-11.12% to 8.51%
Testing data points (34 pts.)	34	29	2.45	-5.21% to 6.91%

For the calculation of the index of contribution for each variable, Equations (4) to (6) are employed according to the weight matrices, \mathbf{w}^1 and \mathbf{w}^2 shown above. The computation process is as follows:

- i. For each hidden neuron k , the absolute value of the hidden-output layer connection weight is divided by the summation of the hidden-output layer connection weight. The Q_k is computed for each neuron as follows:

Heat Transfer Mode	Hidden Neuron 1	Hidden Neuron 2	Hidden Neuron 3	Hidden Neuron 4	Hidden Neuron 5	Hidden Neuron 6
Forced convection	3.18	1.14	1.37	1.05	0.47	0.09
Mixed convection	3.21	2.01	0.50	0.30	1.44	0.12

- ii. For each hidden neuron k , multiply the Q_k by the absolute value of the hidden-input layer connection weight. Then, sum up the values to obtain the P_j for each input variable p_j :

Heat Transfer Mode	Gz	Ra	μ_b/μ_w
Forced convection	2.25	0.38	1.53
Mixed convection	2.20	1.21	1.29

- iii. Compute the index of contribution in percentage by dividing P_j by the sum of the P_j corresponding to each input variable. Finally, the index of contribution for each variable is established as:

Heat Transfer Mode	Gz	Ra	μ_b/μ_w
Forced convection	53.9%	9.2%	36.9%
Mixed convection	46.8%	25.7%	27.5%

From the above table, it can be seen that for the forced convection data, Gz is the most important dimensionless parameter since the forced convection data is all very near the entrance of the tube. On the other hand, Ra is the least important dimensionless parameter since near the tube entrance; the secondary flow effect has not developed yet. For the mixed convection data, Gz is again the most important dimensionless parameter since for laminar heat transfer; the thermal entry length is long. Compared to the forced convection data, Ra in this case is also important since the secondary flow effect has established. For both forced and mixed convection cases, the viscosity ratio is important due to the significant effect of variation of physical properties. Therefore, it can be concluded that the index of contribution calculated based on the proposed method completely agrees with the physical meanings.

CONCLUSIONS

In this study, the factor analysis using ANN proposed by Tam et al. (2006) is applied to the laminar dataset. The data in the laminar region is more complicated since the effects of entrance, buoyancy and variation of properties are important. Graetz number, Rayleigh number and bulk-to-wall viscosity ratio were selected and the percent contribution from each of them was analyzed using the proposed method. It is found that the Gz number is the most important variable in the laminar flow region. Moreover, the Ra number contributes significantly in the mixed convection region. Therefore, the factor analysis

method using ANN can be applied not only in the turbulent but also in the laminar region. Application of this method to more complicated heat transfer problems to further verify its capability is recommended.

REFERENCES

- Ghajar, A. J. and Kim, J., 2006, "Calculation of Local Inside-Wall Convective Heat Transfer Parameters from Measurements of the Local Outside-Wall Temperatures along an Electrically Heated Circular Tube," Heat Transfer Calculations, edited by Myer Kutz, McGraw-Hill, New York, NY, pp. 23.3-23.27.
- Ghajar, A. J. and Tam, L. M., 1994, "Heat Transfer Measurements and Correlations in the Transition Region for a Circular Tube with Three Different Inlet Configurations," Experimental Thermal and Fluid Science, Vol. 8, No. 1, pp. 79-90.
- Ghajar, A. J. and Tam, L. M., 1995, "Flow Regime Map for a Horizontal Pipe with Uniform Heat Flux and Three Different Inlet Configurations," Experimental Thermal and Fluid Science, Vol. 10, No. 3, pp. 287-297.
- Ghajar, A. J., Tam, L. M., and Tam, S. C., 2002, "A New Heat Transfer Correlation in the Transition Region for a Horizontal Pipe with a Reentrant Inlet -Using Artificial Neural Network", Proceeding of the 12th International Heat Transfer Conference, vol. 2, pp 189-194, Grenoble, France, August 18-23, 2002.
- Hornik, K., 1991, "Approximation Capabilities of Multilayer Feedforward Networks," Neural Networks, Vol. 4, No. 2, pp. 251-257.
- Martinelli, R.C., and Boelter, L.M.K., 1942, "The Analytical Prediction of Superposed Free and Forced Viscous Convection in a Vertical pipe", Univ. Calif. Publ. Eng., Vol. 5, No.2, pp. 23.
- Rumelhart, D. E., Hinton, G. E., and Williams, R. J., 1986, "Learning Internal Representations by Error Propagation," Parallel Distributed Processing: Explorations in the Microstructure of Cognition, (Eds: D. E. Rumelhart, and J. L. McClelland) Vol. 1, MIT Press, Cambridge, Mass., pp. 318-362.
- Sieder, E. N., and Tate, G. E., 1936, "Heat Transfer and Pressure Drop in Liquids in Tubes," Ind. Eng. Chem., Vol. 28, pp. 1429-1435.
- Tam, H. K., Tam, S. C., Ghajar, A. J., and Tam, L. M., 2006, "Factor Analysis for Convective Heat Transfer for a Horizontal Tube in the Turbulent Flow Region Using Artificial Neural Network," Proceedings of Tenth international conference on enhancement and Promotion of Computational Methods in Engineering and Science (EPMESC X), pp.657-664, 21-23th of August, 2006, Sanya, Hainan, China.
- Tam, L. M. and Ghajar, A. J., 2006, "Transitional Heat Transfer in Plain Horizontal Tubes," Heat Transfer Engineering, Vol. 27, No. 5, pp. 23-38.